5-13-2017

Surface Mutation Thr34His Facilitates Purification of Haemophilus influenza Carbonic Anhydrase via Metal Affinity Chromatography

Caroline Foley
Providence College

Dr. Kathleen Cornely
Providence College

Surface Mutation Thr34His Facilitates Purification of *Haemophilus influenza* Carbonic Anhydrase via Metal Affinity Chromatography

Received May 13, 2017

Caroline Foley[1], **Dr. Kathleen Cornely**[1,2]

From the Department of Chemistry and Biochemistry, Providence College, Providence, RI, 02918

In order to pursue *Haemophilus influenza* carbonic anhydrase (HICA) as a potential drug target, easy and efficient purification methods must be developed. While immobilized metal affinity chromatography (IMAC) may be used, complications with polyhistidine tags is a concern. Inspired by the endogenous metal affinity of *Escherichia coli* β-carbonic anhydrase (ECCA), we suggest that the generation of histidine clusters on HICA's surface will facilitate its purification by metal affinity chromatography without the potential interference of His-tags. Here we investigate the Thr34His mutation as a method to generate metal affinity in HICA. Since Thr34His is located only 5.3 Å away from His32, the two residues make a vicinal histidine pair that can interact with nickel resin. We report successful generation of Thr34His HICA mutant plasmid via site-directed mutagenesis. To obtain mutant protein for metal affinity chromatography, Thr34His HICA was overexpressed in *E. coli* cells and isolated as a cell lysate with a concentration of 20.2 ± 0.6 mg/mL. Metal affinity chromatography was performed on the sample, and the chromatography fractions were analyzed by SDS-PAGE in order to assess the metal affinity of the mutant. SDS-PAGE revealed that while Thr34His HICA eluted at low 10 mM and 25 mM concentrations of imidazole, 150 mM imidazole was required to fully elute the mutant. These results suggest that through the generation of surface histidine pairs, HICA can be engineered to have metal affinity and thus be easily purified via IMAC.

Carbonic anhydrases (carbonic hydrolase, EC 4.2.1.1) are zinc metalloenzymes that are essential for survival in most mammals, as well as in plants, algae, archaea, and eubacteria (1). Responsible for the interconversion of carbon dioxide and bicarbonate, carbonic anhydrases are involved in maintaining homeostasis in the cell:

$$CO_2 + H_2O \leftrightharpoons HCO_3^- + H^+ \quad (1)$$

At physiological pH, the equilibrium between carbon dioxide and bicarbonate favors the negatively charged bicarbonate species, which is unable to pass through lipid membranes. Carbonic anhydrases convert bicarbonate into carbon dioxide in order to allow transport into the cell, where bicarbonate can be regenerated if needed (for a review, see 1). Through this mechanism, carbonic anhydrase maintains intracellular concentrations of carbon dioxide and bicarbonate that are essential for various enzymatic and cellular processes. Consequently, carbonic anhydrase activity impacts respiration, ion transport, calcification, and biosynthetic reactions in eukaryotes (1). The physiology associated with prokaryotic carbonic anhydrases is less well known.

Carbonic anhydrase activity in bacteria is particularly intriguing though because of its effect on the growth, virulence, and survival of bacterial pathogens (1). *Haemophilus influenza* is a human-respiratory tract pathogen that often causes noninvasive mucosal infections, such as otis media, sinusitis, and conjunctivitis, as well as invasive infections such as meningitis (2). By utilizing carbonic anhydrase, *H. influenza* is able to survive in many conditions including areas of either low or high carbon dioxide concentration (2). Also, interestingly, the β class of carbonic anhydrase predominates in bacteria such as *H. influenza*, but it is not found in mammals where only the α class is found. Due to this unique β isozyme, it may be possible to selectivity target bacterial pathogens in humans, and with the emergence of drug-resistant bacteria, these enzymes are being investigating more thoroughly as potential antibiotic targets (3). In order to pursue these targets, however, developing easy protein purification methods is critical.

Since its introduction as a protein purification technique in 1975 by Porath *et al.*, immobilized metal affinity chromatography (IMAC)[3] has become one of the most widely used affinity chromatography techniques to purify recombinant protein (4). IMAC exploits the affinity of histidine and cysteine residues to transition metal ions such as Ni^{2+} that can be fixed to solid resins via chelating ligands. With the improvement of recombinant

[1]Both authors contributed equally to this work.

[2]To whom correspondences should be addressed: Dept. of Chemistry and Biochemistry, Providence College, 1 Cunningham Squ., Providence, RI 02918. Tel.: 401-865-2866; Email: kcornely@providence.edu

[3]The abbreviations used are: IMAC, immobilized metal affinity chromatography; NTA, nitrilotriacetic acid; ECCA, *Escherichia coli* carbonic anhydrase; HICA, *Haemophilus influenza* carbonic anhydrase; IPTG, isopropyl β-D-1-thiogalactopyranoside; BCA, bicinchoninic acid

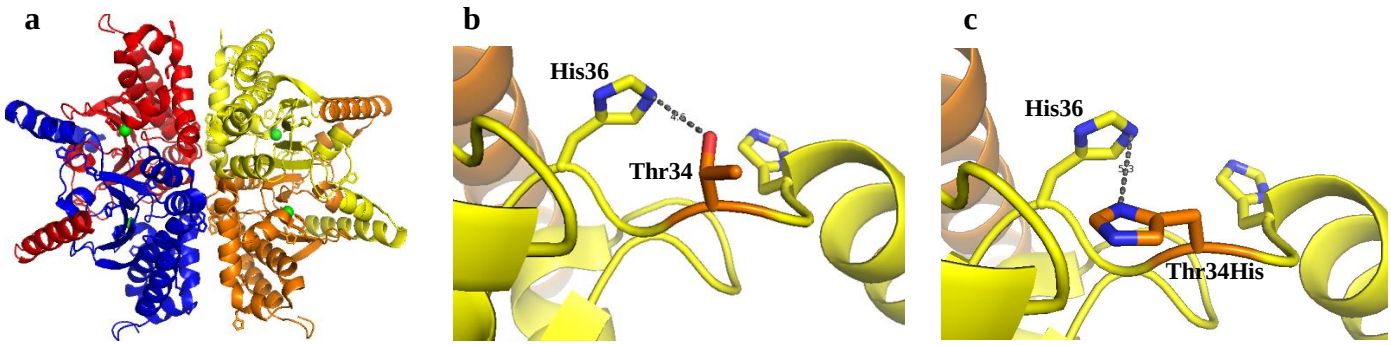

FIGURE 1. **Images of HICA and target residues viewed in PyMOL Molecular Graphics Service System (Version 1.8 by Schrödinger, LLC) using the HICA PDB File 2A8D.** *a*, The dimer of dimers structure of HICA, as well as the zinc active site, is featured in different colors. Several histidine residues are shown along solvent-exposed areas of the protein. *b*, Thr34 is shown on a solvent-exposed surface 4.6 Å away from His36. *c*, When Thr34 is mutated to a histidine, Thr34His is 5.3 Å away from His36 from epsilon nitrogen to delta nitrogen—an optimal distance for vicinal binding to a nickel resin.

techniques and chelating ligands, IMAC can now be used to efficiently purify polyhistidine-tagged proteins in one step (4). However, this purification method becomes problematic when His-tags alter the native structure of a protein, thereby affecting the protein's expression, ability to bind ligands or natural substrates, solubility and/or enzymatic activity. If the native structure cannot be restored by moving the tag to the other terminus, then more extensive purification methods are required (5). His-tags may be removed following purification but this can also be challenging (6). IMAC is further complicated if in addition to the recombinant target protein, native proteins also bind to the column (7).

Escherichia coli β-carbonic anhydrase (ECCA) was discovered to have endogenous metal affinity after it was identified as a common contaminant that is co-purified in IMAC (4). When Ni-NTA[3] chromatography is used to purify protein, there are two available valences on nickel to interact with a pair of histidine residues (5). Since ECCA contains solvent-exposed histidine clusters at the interface between its two dimers, it is not necessary to engineer a polyhistidine tag in order to purify ECCA via IMAC. Residues His72, His122, and His160 on each dimer interact to form vicinal histidine pairs that can stably bind to the nickel ion. The distance between histidine residues in this cluster range from 5 to 7 Å within each chain and 3.5 to 4.5 Å between chains (5). The close distance of these residues allows stable coordination to the nickel.

Hoffman *et al.* recently demonstrated how similar metal affinity can be engineered in *Haemophilus influenza* carbonic anhydrase (HICA) through surface histidine mutations, allowing efficient IMAC purification without the potential interference of polyhistidine tags (5). Although HICA shares 38% identity, quaternary structure, and activity profile with ECCA, as well as a partially conserved histidine cluster (His72, His122, and Arg160), it is unable to bind to nickel without a polyhistidine tag (5). By mutating Arg160 to a histidine residue, and thereby reproducing the histidine cluster in ECCA, Hoffman *et al*. were able to engineer nickel affinity on the surface of HICA. Hoffman *et al*. observed no retention of the wildtype HICA to a Ni-NTA column. However, 190 mM imidazole was required to elute the Arg160His HICA mutant, with ECCA requiring 278 mM imidazole (5). Following these positive results, steady-state kinetic experiments were performed to ensure the Arg160His mutation did not alter the native conformation or activity of HICA, which it did not. These results suggest that the engineering of surface histidine residues may be a more advantageous way to approach IMAC than the tradition method utilizing polyhistidine tags.

Interested in pursuing this hypothesis further, we investigated the metal affinity of the Thr34His HICA mutant. Thr34 was chosen for mutagenesis because it was solvent-exposed and nearby to histidine residues 32 and 36. When the Thr34His mutation in HICA is viewed in PyMOL Molecular Graphics Service System (Version 1.8 by Schrödinger, LLC), Thr34His is only 5.3 Å away from His36 (Fig. 1*c*). Hoffman *et al.* suppose that given the rotational range of motion in histidine residues, an optimal histidine pair for IMAC is between 4 to 7 Å apart (5). With the Thr34His mutation within this distance range to His32, the mutant was pursued. Here we report that the Thr34His mutation in HICA greatly increased the metal affinity of the protein, with 150 mM imidazole needed to elute the mutant from a Ni-NTA column. These results demonstrate that the generation of solvent-exposed histidine pairs in HICA can facilitate its purification by Ni-NTA chromatography.

Results

Selection of the Thr34His mutation using PyMOL–To identify solvent-exposed histidine residues on HICA, the PDB file 2A8D was viewed in PyMOL Molecular Graphics Service System (Version 1.8 by Shrödinger). Using the Mutagenesis tool, residues nearby to surface histidine residues were mutated, and using the

Measurement tool, the distance between wildtype residues and mutant residues were determined. Thr34 was the mutant of choice because of its close proximity (4.6 Å) to His36 (Fig. 1*b*). In addition, Thr34 and His36 are solvent-exposed and are located away from the Zinc active site. Therefore, the mutation Thr34His should not interfere with the activity of the enzyme but could potentially form a vicinal histidine pair with His36 that could bind to a nickel column.

Construction of the Thr34His HICA mutant plasmid– To generate the Thr34His HICA mutant, site-directed mutagenesis was performed using a plasmid containing the HICA gene (see Culture preparation in the Experimental Procedures for complete description of the plasmid). In the first PCR, the three-base mutation was introduced, with the expected product being 287 bp in length. A band of approximately 300 bp was observed on the gel and recovered to be used as a megaprimer in subsequent PCR (Fig. 2*a*). In the second PCR, the entire Thr34His HICA gene was constructed, with the expected product being 883 bp in length. A band of approximately 900 bp was observed and recovered to be used as the forward and reverse primers in a third PCR (Fig. 2*b*). In the third PCR, the entire 4,827 bp plasmid containing the Thr34His HICA gene was synthesized. Sequencing of a section of the HICA gene confirmed that the Thr34His mutation was introduced.

Induced overexpression and extraction of Thr34His HICA–To obtain Thr34His HICA for later analysis, XJb *E. coli* cells were transformed with the mutant plasmid, and liquid cultures were prepared. Overexpression cultures were prepared containing washed and pelleted XJb + Thr34His HICA cells, arabinose, and isopropyl β-D-1-thiogalactopyranoside (IPTG). IPTG induced expression of Thr34His HICA by binding to the lac repressor, allowing the lac operon to bind RNA polymerase and transcribe the downstream Thr34His HICA gene. A cell pellet of 12.749 g was harvested. In order to extract Thr34His HICA from these cells, cell lysis was promoted by freezing and thawing the cells to disrupt the cell membranes. Additionally, arabinose induced the expression of λ-lysozyme, which degraded the cell walls and further induced lysis. The cells were treated with a protease inhibitor and DNase to maintain any protein and degrade any DNA in the cell. A bicinchoninic (BCA) assay was next preformed to determine the concentration of the cell lysate.

BCA Assay–To determine the concentration of the cell lysate, a BCA assay was performed. A standard curve was constructed using BSA standards (Fig. 3). A 1:20 dilution of the cell lysate was prepared in order to be within the absorbance range of the BSA standard curve. A final cell lysate concentration of 20.2 ± 0.6 mg/mL was determined.

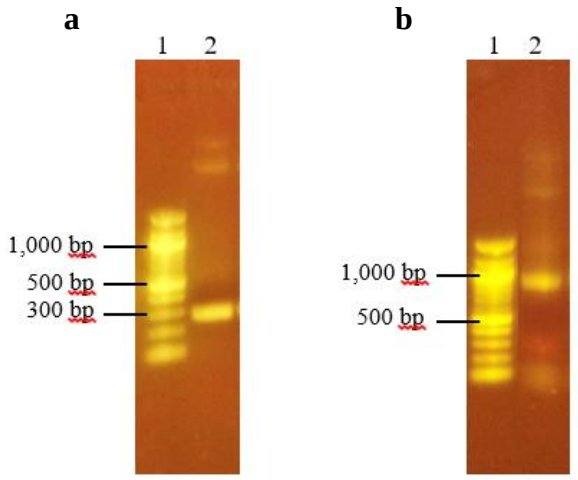

FIGURE 2. **DNA gels verifying the length of the products from the first and second PCR.** *a*, In the first PCR, the Thr34His mutation was introduced and a 287 bp region was amplified. In lane 2, a band of approximately 300 bp is shown, as compared to the ladder in lane 1. *b*, In the second PCR, a 883 bp product encompassing the entire Thr34His HICA gene was amplified. In lane 2, a band of approximately 900 bp is shown, as compared to the ladder in lane 1.

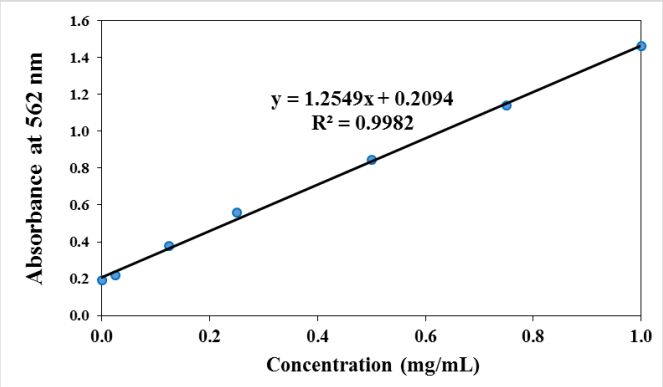

FIGURE 3. **Standard curve for the BCA assay.** To construct this plot, BSA standards were used. From the linear regression of this plot, the concentration of the cell lysate harvested from the overexpression cultures of XJb + Thr34His HICA cells was determined to be 20.2 ± 0.6 mg/mL.

Ni-NTA Chromatography and SDS-PAGE Analysis– To assess whether the Thr34His mutation increases the metal affinity of HICA as compared to WT, Ni-NTA chromatography was performed on the cell lysate and the chromatography fractions were analyzed by SDS-PAGE. According to Hoffman *et al.*, wild-type HICA shows no retention on a Ni-NTA column, while 278 mM imidazole is required to elute ECCA (5). These results were used as standards for our experiment. The elution profile of our chromatography fractions shows increased absorbance values at 280 nm, ranging from 1.0 to 2.2, in the 25 mM, 50 mM, and 100 mM imidazole elution fractions (Fig. 4*a*). In order to determine if these absorbance values are

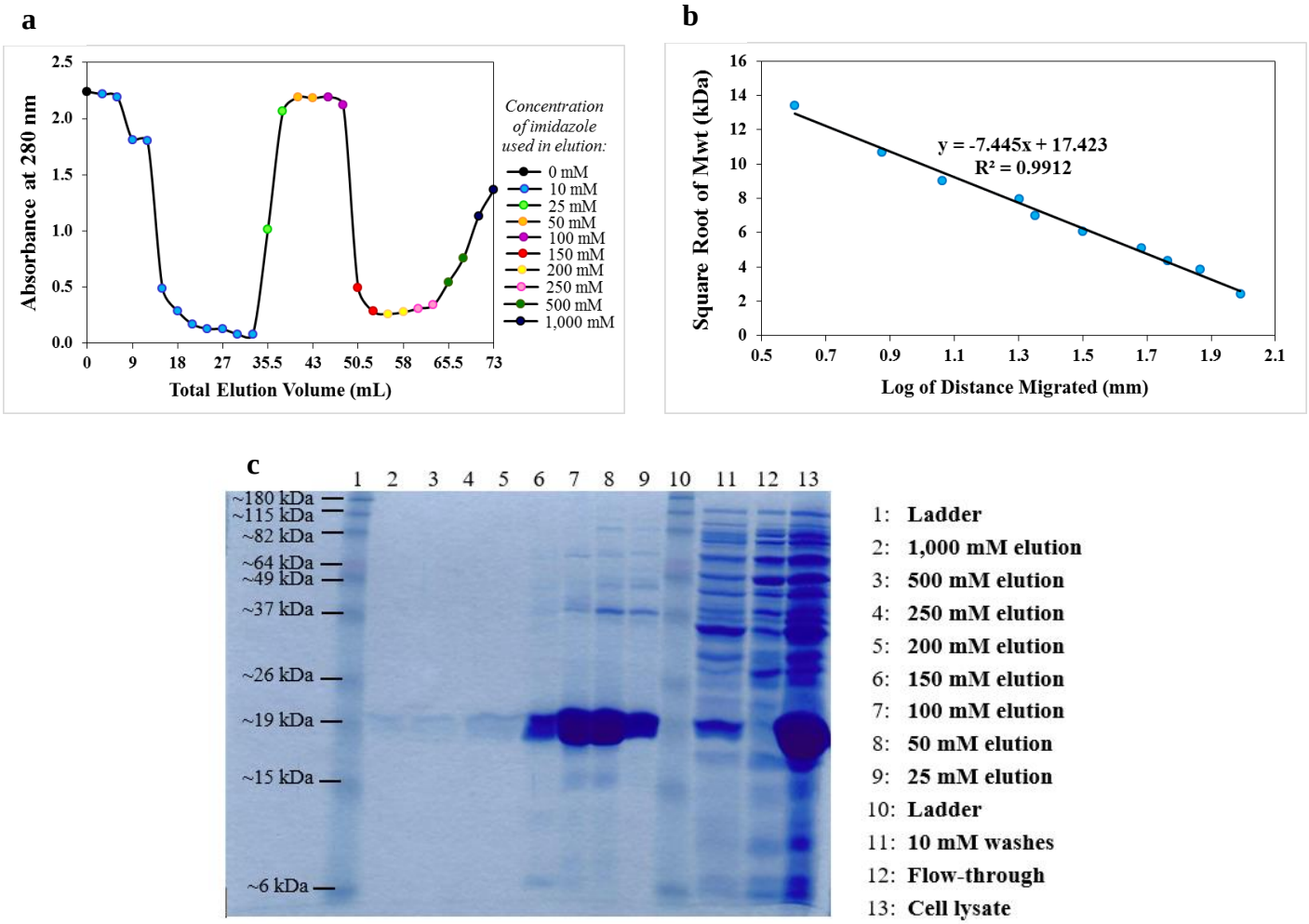

FIGURE 4. **Ni-NTA chromatography and SDS-PAGE analysis shows 20 kDa protein eluting at 25 mM, 50 mM, 100 mM, and 150 mM concentrations of imidazole.** *a*, The elution profile of the chromatography fractions shows increased absorbance ranging from 1.0 to 2.2 in the fractions eluted with 25 mM, 50 mM, and 100 mM imidazole. *b*, A standard curve plotting the square root of the molecular weights of the ladder proteins versus the log of the distance each ladder protein band migrated is shown. From the linear regression of this plot, the molecular weight of protein bands in the gel were determined. *c*, The protein gel shows a prominent 20 kDa band eluting in the 10 mM imidazole washes, as well as in the 25 mM, 50 mM, 100 mM, and 150 mM imidazole elutions.

due to the elution of Thr34His HICA, SDS-PAGE analysis of the cell lysate, flow-through, 10 mM imidazole washes, and elution fractions was performed. Since the cell lysate was treated with SDS, a band size of 25 kDa, corresponding to the Thr34His HICA monomer, was expected. In order to determine the molecular weight of the protein bands in the gel, a standard curve plotting the square root of the molecular weights of the ladder proteins versus the log of the distance each ladder protein band migrated was constructed (Fig. 4*b*). From the linear regression of this plot, the molecular weight of protein in the gel bands were determined. The most prominent band of the cell lysate sample was determined to be 20 kDa (Fig. 4*c*, lane 13). A light 20 kDa band was also shown in the flow-through, with more prominent 20 kDa bands shown in the 10 mM imidazole washes and in the 25 mM, 50 mM, 100 mM, and 150 mM imidazole elutions (Fig. 4*c*). Faint 20 kDa bands were present in the 200 mM, 250 mM, 500 mM, and 1,000 mM imidazole elutions as well (Fig. 4*c*). Bands of 40 kDa length—the same size as the Thr34His HICA dimer—were also present in the cell lysate, flow-through, 10 mM washes, and 25 mM, 50 mM, 100 mM, and 150 mM elution samples (Fig. 4*c*).

Gel filtration–Gel filtration on a representative mutant, Thr200His HICA, that was constructed by the same methods was performed to verify the molecular weight of the untreated cell lysate. The column was calibrated with Blue Dextran, cytochrome c, and N-(2,4-dinitrophenyl)glycine, and a selectivity standard curve plotting k_{av} versus the log of the molecular weight of each protein was constructed (Fig. 5). From the linear regression of this plot, the molecular weight of the cell lysate containing overexpressed Thr200His HICA protein was determined to be 201 kDa—approximately double the size of the expected tetramer.

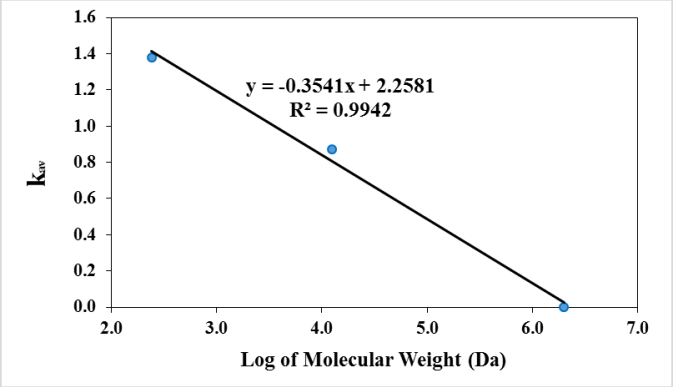

FIGURE 4. **Selectivity curve for gel filtration of Thr200His.** To construct this plot, Blue Dextran, cytochrome c, and N-(2,4-dinitrophenyl)glycine were used as protein standards. From the linear regression of this plot, the molecular weight of the cell lysate containing overexpressed Thr200His HICA protein was determined to be 201 kDa—approximately double the size of the expected tetramer.

Discussion

In continuation of the work of Hoffman *et al.*, we demonstrate how the introduction of surface histidine pairs on HICA can facilitate its purification by Ni-NTA chromatography without the addition of polyhistidine tags. Previously, Hoffman *et al.* engineered nickel affinity on HICA by reproducing the histidine cluster that is present in ECCA (5). We now suggest that only one solvent-exposed histidine pair is required for binding to a Ni-NTA column.

In ECCA, the interactions of residues His72, His122, and His160 on each dimer give the enzyme endogenous metal affinity. In this cluster, histidine residues within the same chain are 5 to 7 Å apart and residues between chains are 3.5 to 4.5 Å apart (5). Due to this close proximity, the histidine residues form pairs that can coordinate to the two open valences on nickel resins in Ni-NTA chromatography and thereby stably bind the protein to the column. Interestingly, Hoffman *et al.* observed that although HICA has a partially conserved histidine cluster consisting of His72, His122, and Arg160, the protein has no nickel affinity and thus, no retention on a Ni-NTA column. When Arg160His is introduced in HICA and the histidine cluster between dimers is restored, the mutant shows affinity for the Ni-NTA column, with 190 mM imidazole required to elute the protein (5). Although ECCA requires higher concentrations of imidazole (278 mM at the peak of elution) to be eluted, these results suggest that metal affinity can be engineered in HICA via the generation of histidine clusters (5).

In order to determine the minimum number of histidine pairs that are needed to bind HICA to a Ni-NTA column, the previously published crystal structure of HICA was viewed in PyMOL Molecular Graphics Service System (Version 1.8 by Schrödinger, LLC) and potential histidine pairs were considered (8). In an effort to generate a vicinal pair that could bind to a nickel column, residues nearby to solvent-exposed histidine residues were mutated and the distance between the two residues were calculated. Thr34His was pursued due to its solvent-exposed location 5.3 Å away from His36 (Fig. 1*b*). Considering the rotational range of motion of histidine residues, we suspected that Thr34His and His36 could form a vicinal pair and bind to a nickel resin.

Thr34His HICA was successfully constructed and expressed using site-directed mutagenesis on a plasmid designed as an expression vector for HICA. DNA gels following the first and second PCR confirmed that products of the expected length were synthesized, and following the construction of the entire mutant plasmid, sequencing confirmed that the Thr34His mutation had been introduced in HICA (Fig. 2). The mutant protein was overexpressed and extracted as a cell lysate to be tested for metal affinity via Ni-NTA chromatography.

SDS-PAGE of the chromatography fractions showed prominent 20 kDa bands, correlating to the 25 kDa Thr34His HICA monomer, in the 10 mM imidazole washes, as well as in the 25 mM, 50 mM, 100 mM, and 150 mM imidazole elutions (Fig. 4*c*). Although the determined molecular weight of the protein was low, the presence of 40 kDa bands correlating to the dimer of Thr34His HICA, corroborated that the 20 kDa bands were monomer protein. Despite some Thr34His HICA elution in the washes, significant amounts of protein were retained on the column until the complete elution by 150 mM imidazole. The faint 20 kDa protein bands in the 200 mM, 250 mM, 500 mM, and 1000 mM imidazole elution fractions were deemed insignificant. These results suggest that through the introduce of a surface histidine pair, enhanced metal affinity can be engineered in HICA, with Thr34His HICA requiring 150 mM imidazole for elution compared to no retention for the WT HICA as observed by Hoffman *et al.* (5).

In order to confirm our results, though, Ni-NTA chromatography should be performed on WT HICA and ECCA as controls. If Thr34His HICA then does not exhibit enhanced metal affinity, the chromatography elutions may need to be adjusted. Greater elution volumes at each imidazole concentration, as well as a more gradual increase in these concentrations, will provide a more exact determination of the metal affinity of Thr34His HICA. However, the current results suggest that only one solvent-exposed histidine pair is required in HICA for its binding to a Ni-NTA column.

Gel filtration on a representative mutant, Thr200His HICA, was also performed to further confirm that the overexpression and extraction protocol was successful. Although a 201 kDa molecular weight—twice the size as the tetramer was determined, these results do not negate the expression of the protein. Rather, Thr200His HICA tetramers appear to have associated to form an octamer complex. The introduced surface mutation may have altered the three-dimensional structure of the protein to promote the formation of this octamer. To determine whether this has also occurred in the Thr34His HICA mutant, gel filtration should be performed on Thr34His HICA.

Also in the future, kinetic experiments should be performed to ensure that the Thr34His mutation does not alter the activity of HICA. Hoffman *et al.* performed these studies on Arg160His HICA and determined no significant change in activity (5). Since Thr34 is far from the zinc active site, we do not suspect that our mutant will affect the activity. The active site is comprised of a zinc ion coordinated to Cys42, Asp44, His98, and Cys101 (9). In order to catalyze CO_2 into HCO_3^-, CO_2 forms hydrophobic interactions with residues along this active site. Here, CO_2 is susceptible to nucleophilic attack by a zinc-bound hydroxide ion that is positioned in place by Asp44. The Gln 151 residue on a neighboring monomer stabilizes the formation of bicarbonate via hydrogen bonding. HCO_3^- is then released from the active site when it exchanges its coordination to zinc with water. Loss of a hydrogen atom in water regenerates the zinc-bound hydroxide ion (9). Since Thr34 is not involved in this mechanism, as it is positioned away from the active site, we do not suspect the Thr34His mutation with affect the activity of HICA (Fig. 1*c*). In future experiments, we hope to confirm this.

Additionally, we would like to mutate the histidine cluster in ECCA and reexamine its affinity for Ni-NTA columns. If ECCA maintains its strong affinity, requiring approximately 278 mM imidazole for elution, then we can investigate what other factors contribute to its metal affinity. This will provide us more structure-function information that we can use to increase the metal affinity of HICA.

Thus far, we have determined that the introduction of the Thr34His mutation in HICA increases the metal affinity of the protein as compared to WT HICA. Thr34His HICA required 150 mM imidazole for complete elution from a Ni-NTA column, whereas WT HICA was not retained on the column (5). These results suggest that only one solvent-exposed histidine pair is needed for easy purification by IMAC without the potential interference of polyhistidine tags.

Experimental Procedures

Culture preparation–LB medium (1% tryptone, 0.5% yeast extract, 1% NaCl, 100 μg/mL ampicillin) was inoculated with a single colony of obtained DH5α *E. coli* cells that had been transformed with plasmid DNA containing the HICA, ampicillin-resistance, lac repressor, lac promoter, and lac operon genes. The liquid culture was incubated in a roller drum for 24 hours at 37 ºC.

Plasmid minipreparation–A plasmid minipreparation of pHICA plasmid from the liquid culture of DH5α *E. coli* cells was performed using the Zyppy Plasmid Miniprep Kit (Zymo Research). The manufacturer's instructions were followed, except that the Zyppy TE Elution Buffer (10 mM Tris, 0.1 mM EDTA, pH 8.5) was warmed to 50 ºC and after the column was treated with Elution Buffer, the sample was incubated for 10 min at room temperature before elution.

Site-directed mutagenesis–The mutation Thr34His was introduced to the HICA gene using site-directed mutagenesis (10). The following primers, synthesized by Integrated DNA Technologies (IDT), were used to amplify the mutation: the forward PhiQC primer, 5'-CACTGCATAATTCGTGTCGCTCAAGG-3' and the reverse mutant primer with the mutant bases underlined, 5'-AAGGTAATGTGGGTGTTGATGATC-3'. PCR was performed in a 25 μL mixture using 110 ng of the template pHICA DNA, 2.5 nmol of each primer, 5 nmol of dNTPs, and 1 U of Phusion High-Fidelity DNA Polymerase (Thermo Scientific) in Phusion HF Reaction Buffer (Thermo Scientific). The thermocycler was programed for touchdown PCR (11, 12) as follows: initial denaturation at 95 ºC for 2 min; 40 cycles at 95 ºC for 30 s, 65 ºC for 30 s (decreasing by 0.5 ºC each cycle), and 72 ºC for 30 s; and extension at 72 ºC for 10 min. Gel electrophoresis was performed for 40 min at 100 V using a 1.5% agarose gel in TAE buffer (40 mM Tris, 20 mM acetic acid, 1 mM EDTA, pH 7.6). The gel was mixed with SYBR Safe DNA Gel Stain (0.01% (v/v)) in order to visualize the bands. An expected band size of approximately 300 base pairs was observed, and the DNA was recovered using the Zymo gel extraction kit. The manufacturer's instructions were followed, except that the Elution Buffer (10 mM Tris, 0.1 mM EDTA, pH 8.5) was warmed to 50 ºC and after the column was treated with 6 μL of the Elution Buffer, the sample was incubated for 10 min at room temperature before elution.

To amplify the entire HICA gene containing the

mutation Thr34His, a second PCR was performed using the product of the first PCR as a forward megaprimer and the reverse primer Phi2X, with the sequence: 5'-AGCTTGCATGCCTGCAGTTATTAT-3' (IDT). PCR was performed in a 25 µL mixture using 110 ng of the template pHICA DNA, 3 µL of the megaprimer, 25 pmol of Phi2X, 5 nmol of dNTPs, and 1 U of Phusion High-Fidelity DNA Polymerase (Thermo Scientific) in Phusion HF Reaction Buffer (Thermo Scientific). The thermocycler was programmed for touchdown PCR as described above with the exception of a longer cycle extension time of 1 min at 72 ºC. Gel electrophoresis was performed as described above, except a 1% agarose gel in TAE buffer was used. An expected band size of approximately 900 base pairs was observed. The DNA was recovered as previously described, except that the sample was eluted with 12 µL of the elution buffer.

To amplify the entire pHICA plasmid containing the mutation Thr34His, a third PCR was performed. PCR was performed in a 25 µL mixture using 110 ng of the template pHICA DNA, 5 µL of the product of the second PCR (to be used as both the forward and reverse primer), 5 nmol of dNTPs, and 1 U of Phusion High-Fidelity DNA Polymerase (Thermo Scientific) in Phusion HF Reaction Buffer (Thermo Scientific). The thermocycler was programmed for classical PCR as follows: initial denaturation at 95 ºC for 2 min; 30 cycles at 95 ºC for 1 min, 60 ºC for 1 min, and 72 ºC for 5 min; and extension at 72 ºC for 10 min.

Preparation of competent cells–DH5α *E. coli* cells were made competent using the Mix & Go *E. coli* Transformation Kit & Buffer Set (Zymo Research) and then immediately tested for competency. The manufacturer's instructions were followed with a transformation efficiency of 2.5×10^3 cfu/µg achieved.

Transformation of mutant pHICA–Competent DH5α *E. coli* cells were transformed with pHICA Thr34His DNA that was generated in the third round of PCR. The product from the third PCR was first treated with 20 U of Dpn1 enzyme and incubated for 3 hours at 37 ºC in order to degrade any remaining template pHICA DNA from the sample. Dpn1 only digested template DNA because the enzyme recognizes methylated adenine nucleotides, which are only present in the bacterial DNA. The PCR product is not methylated and was not affected in the digest. Following the digest, the remaining pHICA Thr34His DNA was then used to transform DH5α *E. coli* cells. To do this, 5 µL of the digested PCR sample was added to 100 µL of competent DH5α *E. coli* cells. The sample was incubated for 45 minutes on ice and then plated on pre-warmed ampicillin resistant LB culture plates (1% tryptone, 0.5% yeast extract, 1% NaCl, 100 µg/mL ampicillin). The plates were incubated for 22 hours at 37 ºC. Three days later, plates were re-streaked and incubated for 24 hours at 37 ºC.

Sequencing–Samples for sequencing were prepared by first inoculating liquid cultures of LB medium with DH5α *E. coli* cells transformed with pHICA Thr34His DNA. The liquid cultures were incubated in a roller drum for 24 hours at 37 ºC. A plamid minipreparation was performed for each culture by using the Zyppy Plasmid Miniprep Kit (Zymo Research) as described previously. A 20 µL sequencing sample in TE buffer (10 mM Tris, 1 mM EDTA) was prepared containing 2.0 µg of the pHICA Thr34His DNA and 30 pmol of the pRRXseqforward primer, with the sequence: 5'-GCTCGTATAATGTGTGGAATTG-3' (IDT). The sequencing was performed by the CCIB DNA Core Facility at Massachusetts's General Hospital (Cambridge, MA).

Overexpression of HICA Thr34His protein–To prepare for protein overexpression, XJb *E. coli* cells (Zymo Research) were transformed with pHICA Thr34His DNA and liquid cultures were grown as described previously. The liquid cultures were pelleted at 8,000 × g for 5 minutes. The cells were re-suspended in 10 mL of LB medium and added to a 2.5 L Tunair flask containing 900 mL TB nutrient solution (2.67% w/v yeast extract, 1.33% w/v tryptone, 0.5% glycerol), 100 mL TB buffer solution (0.89 M potassium phosphate, pH 7.5), and 3 mM arabinose. The culture was incubated with vigorous shaking for four hours at 37 ºC until the OD_{600} was between 0.60 and 1.0. To induce expression of HICA Thr34His protein, isopropyl β-D-1-thiogalactopyranoside was added to the culture to obtain a 0.5 mM concentration. The cells were incubated with vigorous shaking at 280 rpm for 21 hours at 37 ºC. The cells were harvested by centrifuging four 250-mL portions of the culture at 8,000 × g for 10 min. The resulting cell pellet was 12.749 g.

Cell lysis–To induce physio-chemical stress on the cell membrane and cause cell lysis, the pellet described above was frozen at -80 ºC and then thawed and resuspended in 38 mL (3 mL/g of cells) of lysis buffer (20 mM Tris, 100 mM NaCl, pH 8.0). One Pierce Protease Inhibitor Mini Tablet (Thermo Scientific) and 1 mg of DNAse (Sigma Aldrich) was dissolved in the solution. The sample was incubated with vigorous shaking for one hour at 37 ºC. The cells were then pelleted at 35,000 × g for 30 minutes, and the pellet was discarded. The supernatant was

centrifuged for an additional 15 min at 35,000 × g and then stored at -20 ºC.

BCA assay–To determine the protein concentration of the cell lysate, a BCA assay (13) was performed using the Pierce BCA Protein Assay Kit (Thermo Scientific). The manufacturer's instructions were followed. A 1:20 dilution of sample was required for a sample absorbance within the range of standard absorbance values. The absorbance was measured at 562 nm using a Cary 50.

Dialysis–Before Ni-NTA chromatography was performed, the cell lysate was dialyzed with the PURG0015 Pur-A-Lyzer Mega Dialysis Kit (Sigma Aldrich) to remove Tris from the sample. Tris was removed because it can bind to Ni-NTA columns and may interfere with the binding of the target protein Thr34His HICA. The manufacturer's instructions were followed in a phosphate-buffered saline (PBS) solution (20 mM sodium phosphate, 300 mM NaCl, pH 7.4). The Pur-A-Lyzer tube was loaded with 10 mL of the cell lysate (202 mg) and dialyzed for 16 hours in 2.5 L of PBS buffer, followed by 3 hours in fresh buffer.

Ni-NTA chromatography–Ni-NTA chromatography was performed to assess the binding capability of Thr34His HICA (4). An equilibration matrix was prepared by adding 4 mL of a HisPur Ni-NTA Resin (Thermo Scientific) ethanol slurry with a 2 mL bed volume and a 120 mg binding capacity. The mixture was centrifuged for two minutes at 1,286 × g, and the supernatant was discarded. The pellet was then re-suspended in 3 mL of PBS equilibration buffer, mixed by inversion, and centrifuged for another 2 minutes at 1,286 × g. The packed resin was treated with 5 mL of the thawed cell lysate (101 mg) and incubated for one hour with shaking at 4 ºC. The lysate-treated resin was loaded into a column and the flow-through was collected. The column was then repeatedly washed with 3 mL volumes of wash buffer (10 mM imidazole in PBS buffer) until the OD_{280} was below 0.01. Protein was eluted using two 2.5 mL column volumes of the following solutions of imidazole in PBS buffer: 25 mM, 50 mM, 100 mM, 150 mM, 200 mM, 250 mM, 500 mM, 1000 mM imidazole. The cell lysate, flow-through, combined wash fractions, and elution fractions at each concentration of imidazole were next analyzed by SDS-PAGE.

SDS-PAGE analysis–The Ni-NTA chromatography column fractions were analyzed by SDS-PAGE analysis to assess how strongly Thr34His HICA binds to a Ni-NTA column. Laemmli's procedure (14) was followed with these exceptions: a 12.5% acrylamide separating gel was prepared and only 0.3% of *N,N,N',N'*-tetramethylethylenediamine was used to catalyze the polymerization of the stacking gel. Samples of the cell lysate, flow-through, 10 mM imidazole washes, and elution fractions at each concentration of imidazole were prepared according to Laemmli as well with the following exceptions: the samples contained 2mM DTT, 0.005% bromophenol blue, and 1% β-mercaptoethanol. Before loading the samples onto the gel, the samples were incubated at 100 ºC for three minutes. Gel electrophoresis using the reservoir buffer described by Laemmli was performed overnight for 17 hours at 55 mamps through the stacking gel and approximately 4 mamps through the separatory gel. The gel was stained in 0.025% Coomassie Blue R-250 stain (40% methanol, 7% acetic acid) for approximately five hours and de-stained by initially microwaving the gel submerged in water and then leaving the gel in destaining solution (40% methanol, 7% acetic acid, 3% glycerol) for six days. Once destained, the gel was dried under vacuum in a gel dryer for 2 hours at 80 ºC and then for 1 hour at room temperature.

Gel filtration–Gel filtration was performed on a representative mutant, T200H HICA to confirm the molecular weight of the tetramer. Sephadex G-200 resin (Pharmacia) was used and GE Healthcare's instructions for Sephadex media were followed. The column was equilibrated with PBS buffer and calibrated with a 1 mL sample containing 6 mg Blue Dextran, 6 mg cyctochrome c, and 6mg DNP-Glycine in 10 mM acetic acid at pH 5. A flow rate of 0.5 mL/min was used, and effluent was monitored at 280 nm and fractions collected. A 3-mL sample of a cell lysate containing overexpressed T200H (33.9 ± 0.1 mg/mL) was run through the column. A selectivity curve of the standards was constructed, from which the molecular weight of T200H HICA was determined to be 201 kDa.

Acknowledgements—We gratefully acknowledge Dr. Katherine Hoffman (Department of Chemistry, California Lutheran University, Thousand Oaks, CA) for allowing us to pursue her research and for suppling us with the DH5α *E. coli* cells transformed with the plasmid HICA DNA. We would also like to thank Dr. Brett Pellock and Dr. Nicanor Austriaco, O.P. (Department of Biology, Providence College, Providence, RI) for many helpful conversations, as well as the librarian staff at Providence College for their assistance. In addition, thank you to Patrick Tate from Providence College for supplying us with the Thr200His HICA mutant. Finally, thank you to the Department of Chemistry and Biochemistry, as well as the Department of Biology, at Providence College for their funding and resources.

References

1. Smith, K. S., and Ferry, J. G. (2000) Prokaryotic carbonic anhydrases. FEMS Microbiol. Rev. **24**, 335-366.
2. Langereis, J. D., Zomer, A., Stunnenberg, H. G., Burghout, P., and Hermans, P. W. M. (2013) Nontypeable *Haemophilus influenzae* carbonic anhydrase is important for environmental and intracellular survival. J. Bacteriol. **195**, 2737-2746.
3. Supuran, C. T. (2011) Bacterial carbonic anhydrases as drug targets: toward novel antibiotics? Front. Pharmacol. **2**:34, 1-6.
4. Block, H., Maertens, B., Spriestersbach, A., Brinker, N., Kubicek, J., Rabis, R., Labahn, J., and Schäfer, F. (2009) Immobilized-metal affinity chromatography (IMAC): A review. Methods Enzymol. **463**, 439-473.
5. Hoffman, K. M., Wood, K. M., Labrum, A. D., Lee, D. K., Bolinger, I. M., Konis, M. E., Blount, A. G., Prussia, G. A., Schroll, M. M., and Watson, J. M. (2014) Surface histidine mutations for the metal affinity purification of a β-carbonic anhydrase. Anal. Biochem. **458**, 66-68.
6. Mooney, J. T., Fredericks, D., Christensen, T., and Heam, M. T. W. (2014) Removal of cleavage slow points from affinity tage used in the IMAC purification of recombinant proteins. Biotechnol. J. 9, 1023-1032.
7. Bolanos-Garcia, V. M., and Davies, O. R. (2006) Structural analysis and classification of native proteins from E. coli commonly co-purified by immbobilised metal affinity chromatography. Biochim. Biophys. Acta. **1760**, 1304-1313.
8. Cronk, J. D., Rowlett, R. S., Zhang, K. Y. J., Tu, C., Endrizzi, J. A., Lee, J., Gareiss, P. C., and Preiss, J. R. (2006) Identification of a novel noncatalytic bicarbonate binding site in eubacterial β-carbonic anhydrase. Biochemistry. **45**, 4351-4361.
9. Rowlett, R. S. (2010) Structure and catalytic mechaniam of the β-carbonic anhydrases. Biochim. Biophys. Acta. **1804**, 362-373.
10. Barik, S. (1996) Site-directed mutagenesis in vitro by megaprimer PCR. Methods Mol Biol. **57**, 203-215.
11. Don, R. H., Cox, P. T., Wainwright, B. J., Baker, K., and Mattick, J. S. (1991) 'Touchdown' PCR to circumvent spurious priming during gene amplification. Nucleic Acids Res. **19**, 4008.
12. Roux, K. H., and Hecker, K. H. (1997) One-step optimization using touchdown and stepdown PCR. Methods Mol Biol. **67**, 39-45.
13. Smith, P. K., Krohn, R. I., Hermanson, G. T., Mallia, A. K., Gartner, F. H., Provenzano, M. D., Fujimoto, E. K., Goeke, N. M., Olson, B. J., and Klenk, D. C. (1985) Measurement of protein using bicinchoninic acid. Anal Biochem. **150**, 78-83.
14. Laemmli, U. K. (1970) Cleavage of structural proteins during the assembly of the head of bacteriophage T4. Nature. **227**, 660-685.